Title
ON THE TREATMENT OF A TWO-DIMENSIONAL FISSION MODEL WITH COMPLEX TRAJECTORIES

Author
Ring, P.

Publication Date
1977-06-01

Submitted to the
Nuclear Physics

LBL-6538
Preprint

ON THE TREATMENT OF A TWO-DIMENSIONAL FISSION MODEL WITH COMPLEX TRAJECTORIES

P. Ring, H. Massmann, J. O. Rasmussen

June 1977

Prepared for the U. S. Energy Research and
Development Administration under Contract W-7405-ENG-48

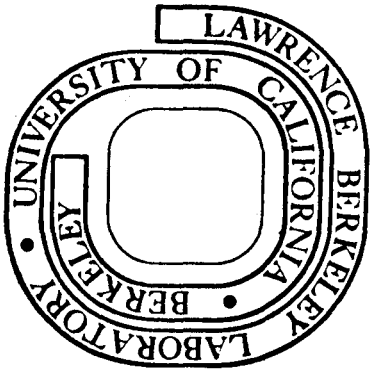

DISCLAIMER

ON THE TREATMENT OF A TWO-DIMENSIONAL FISSION MODEL WITH COMPLEX TRAJECTORIES

P. Ring
Physik-Department, Technische Universität München
8046 Garching, Germany

H. Massmann[+]
Hahn-Meitner-Institut für Kernforschung
Glienicker Str. 100, 1 Berlin 39

J. O. Rasmussen
Lawrence Berkeley Laboratory, University of California
Berkeley, CA 94720

Abstract: The tunneling problem through multi-dimensional fission barriers is studied on a simple two-dimensioan model. The uniform semi-classical approximation with complex classical trajectories is applied and the results are compared with an exact quantum-mechanical solution by a coupled channel calculation. The results show very good agreement.

[+]Present address: Facultad de Ciencias, Universidad de Chile, Santiago, Chile

1. Introduction

The theoretical description of the fission process is one of the oldest problems in nuclear physics. It involves collective and single-particle aspects. Much work has been done to understand this process and many aspects have been clarified, but a unified theoretical description has not yet been given. We will not comment here on all the knowledge one has gained up to now in understanding this process, but refer to the literature, especially to the review article of M. Brack et al./1/ and the references given therein.

Most theories start with a suitable choice of collective coordinates $q_1 \ldots q_f$. One of them is always the fission coordinate which corresponds at the beginning of the fission process to some deformation parameter and goes over, after the fission process, into the distance between the separated fragments. However, to describe the essential behaviour of the nucleus during the fission process one needs further parameters to describe other collective degrees of freedome such as other deformations, the mass asymmetry, or the pairing correlations.

The next step is then the determination of a collective Hamiltonian in these variables. A fully quantum-mechanical way to find such a Hamiltonian is to use the method of generator coordinates. Proposed by Hill and Wheeler/2/ and extended in the following years in many different ways /3-6/, it yields a collective quantum-mechanical Hamiltonian, which is quadratic in the momenta corresponding to the collective coordinates, and has the form:

$$H(q_1 \ldots q_f) = -\frac{\hbar^2}{2} \sum_{i,j}^{f} \frac{1}{\sqrt{g}} \frac{\partial}{\partial q_i} \sqrt{g} \left(M(q_1 \ldots q_f)\right)^{-1}_{ij} \frac{\partial}{\partial q_f} + V(q_1 \ldots q_f) \quad (1)$$

where $g = \det(g_{ik})$ and where $g_{ik}(q_1 .. q_f)$ is the metric tensor of the curvelinear coordinates $q_1 \ldots q_f$. The inertial tensor M_{ik} and the potential energy V depend on these coordinates. Following ref./3-6/ one is in principle able to derive M_{ik} and V from a microscopic Hamiltonian. However, up to now it is only for the case of anharmonic vibrations that one has calculated mass parameters and potential energy surfaces in that way.

For the fission process one usually uses a mixed microscopic-macroscopic method. The energy surfaces are taken from the liquid drop model and shell corrections are added using the Strutinsky method /7/. The mass parameters are obtained from the cranking formula. The energy surfaces calculated using this method are able to explain many features of the fission process. However, not much is known up to now about the mass parameters. Some calculations show a strong dependence on the coordinates q_i, a fact which certainly will influence the fission process.

Once the mass parameters and the potential from such a mixed microscopic-macroscopic method are known, one has to requantize the Hamiltonian. The same has to be done if one starts from the Adiabatic Time-Dependent Hartree-Fock approach /8,9/.

This requantization is certainly not unique and presents additional open problems, with which we will not be concerned with in this paper.

The third step in the solution of the fission problem is to solve the Schrödinger equation in the coordinates $q_1 \ldots q_f$ which results from the Hamiltonian (1). In this paper we consider only this part of the problem. We assume to know a quantum mechanical Hamilton operator H in the coordinates $\{q_i\}$ which corresponds to a classical Hamilton function H in the variables $\{q_i\}$ and the conjugate momenta $\{p_i\}$:

$$H(p_1 \ldots p_f, q_1 \ldots q_f) = \frac{1}{2} \sum_{ij}^{f} \left(M(q_1 \ldots q_f)\right)^{-1}_{ij} p_i p_j + V(q_1 \ldots q_f). \quad (2)$$

So we are left with a multidimensional barrier penetration problem. This problem has been investigated by many groups introducing more or less drastic approximations.

The oldest method used to calculate fission half lives is the one-dimensional WKB method /10/. In the multidimensional energy surface a one-dimensional path is determined which usually goes along the bottom of the fission valley. The Schrödinger equation is transformed to a one-dimensional equation by using only a coordinate along this path. The penetrability is then obtained using the one-dimensional WKB formula:

$$P = \exp\left\{ -2 \int_{\sigma'}^{\sigma''} \sqrt{\frac{2M(\sigma)}{\hbar^2}(V(\sigma)-E)}\, d\sigma \right\} \tag{3}$$

where σ' and σ'' are the turning points determined by $V(\sigma) = E$. For thick barriers and low energies this is an excellent approximation to the one-dimensional Schrödinger equation. For higher energies close to the barrier top this formula has been improved by P. Fröman and N. Fröman /11/ and Jeffreys /12/ so that one has a well-working method in the one-dimensional case.

For the one-dimensional barrier penetration problem, eq.(3) can also be obtained by minimizing the classical action/13/

$$S = \int_{q'}^{q''} p\, dq \tag{4}$$

between the turning points q' and q". This idea has been generalized by the Pauli-Strutinsky group/1/ to the multi-dimensional case. They find the fission trajectory in the multi-dimensional coordinate space by minimizing the action

$$S = \int_{q'}^{q''} \sum_i p_i\, dq_i = \int_{\sigma'}^{\sigma''} \sqrt{2 \sum_{ij} M_{ij} \frac{\partial q_i}{\partial \sigma} \frac{\partial q_j}{\partial \sigma} (E - V(\sigma))}\, d\sigma \tag{5}$$

where σ is some arbitrary parameter along a trajectory $q(\sigma)$. The variation includes all possible trajectories which conserve the energy along the varied path. σ' and σ'' are again the turning points defined by $V(\sigma) = E$. The tunneling probabi-

lity is then given in the usual way by

$$P = \left| e^{i \cdot S} \right|^2 = e^{-2\Im S} \qquad (6)$$

The trajectory so obtained usually does not follow the steepest descent of the potential and does not lead through the extremel points of the deformation energy. It should also be noted that the entrance (σ') and exit point (σ'') are determined in such a way that the action is also stationary against the variation of these end-points. σ' is usually chosen to lie 0.5 MeV (zero point energy) above the bottom of the well; σ'' has to lie on the energy contour with the same energy.

The action determined by this method is a complex solution of the classical Hamilton-Jacobi equation/13/. In that sense the corresponding trajectory is a classical trajectory. One problem is the matching of these trajectories under the barrier to the classical allowed trajectories for $E > V$ which correspond to oscillations in the local minimum of the fissioning nucleus. In the method of Pauli and Strutinsky/1/ there is no connection between the motion under the barrier and the motion outside of the barrier and therefore the problem of the zero-point energy is not handled in a consistent way.

In this paper we consider a method which was originally proposed in theoretical chemistry field by Miller /14-16/ and by Marcus /17,18/, and which allows a consistent semi-classical description of the multi-dimensional barrier penetration problem.

Using this method, one is able to calculate transition probabilities not only from the ground state of the fissioning nucleus to the ground state of the separated system , but also to excited states, as well as all other transition probabilities starting from excited states.

There exists a different attempt to solve the problem quantum-mechanically. H. Hofmann /19/ introduced an harmonic approximation for the potential perpendicular to the fission path. Adding the zero-point energy of this motion to the potential along the fission path, he decomposed the Hamiltonian in an adiabatic part and a remainder. The adiabatic part corresponds to a one-dimensional barrier penetration problem. Its solution yields "distorted" waves. The remainder is treated in the Distorted Wave Born Approximation (DWBA). As we will see shortly in a model calculation, this method is certainly applicable for transitions from the ground state of the fissioning nucleus to the ground state of the separated system, but not for transitions between excited states where the coupling to other transitions is very strong.

In the present paper we investigate the problem on a simple two-dimensional model. This model is introduced and discussed in section 2. In section 3 we give a method to find the exact fully quantum-mechanical solution. Since this method turns out to be too complicated as to be applicable for realistic fission barriers, we discuss a semi-classical approximation in section 4. In section 5 finally both methods are compared.

Some aspects of this work were presented earlier in a review article for the Soviet Journal of Particles and Nuclei.

2. The two-dimensional fission model.

We start with the Hamiltonian (1) for two dimensions (f=2). In ref. 19) it is shown that one can always find a coordinate transformation $x = x(q_1, q_2)$, $y = y(q_1, q_2)$ which has the following properties:

(i) The off-diagonal components of the inertial tensor expressed in the new coordinates vanish,

(ii) The trajectory y=0 defines a path of minimal energy.

In this paper we go a step further and neglect the coordinate dependence of the inertial parameters m_x and m_y. This is certainly not fulfilled in a realistic fission process. But since we do not know much about this dependence and are more interested in the methods to solve the barrier penetration problem, it is worthwhile to start

with the simplest case. On the other hand, both methods which we describe in the next sections can easily be generalized to include a coordinate dependence in the inertial parameters. We therefore start with the following Hamiltonian:

$$\hat{H} = -\frac{\hbar^2}{2m_x}\frac{\partial^2}{\partial x^2} - \frac{\hbar^2}{2m_y}\frac{\partial^2}{\partial y^2} + V(x,y) \qquad (7)$$

According to (ii) one has $\frac{\partial}{\partial y} V(x,y)\Big|_{y=0} = 0.$

The potential along the fission valley V(x,y = 0) has in a typical case a shape like the one shown in fig. 1. Before fissioning the system sits in the local minimum at $x = x_o$; $x = x_{sc}$ shall be the scission point (that is, the place where the nucleus breaks into two fragments). The system, in order to fission, has to penetrate the potential barrier from x_o to x_1.

In order to be able to solve the problem, we introduce further simplifications:

(i) We assume that the y-motion, which is perpendicular to the fission path, allows only bound states.

(ii) V(x,y) shall be independent of x for large positive and negative x-values. This is obviously not true for the potential in fig. 1. This simplification allows us to calculate only the penetrability through the two-dimensional barrier. To get the decay probability (or the life time) one has to multiply with the frequency of the oscillations in x-direction in the local minimum $x = x_o$.

This assumption is usually made in calculating fission half-lives. However, up to now it has not yet been investigated if it is also possible for multi-dimensional problems.

(iii) There shall be no coupling between the two degrees of freedom for $|x| \to \infty$.

The actual calculations were carried out with a barrier of Gaussian shape ($f(z)=e^{-z^2}$) or an Eckard shape ($f(z)=\cosh^{-2}(z)$) and a quadratic y-dependence with variable width:

$$V(x,y) = V_o \cdot f\left(\frac{x}{a}\right) + \frac{1}{2} C \cdot \left(1 + \alpha \cdot f\left(\frac{x}{a}\right)\right) \cdot y^2 \quad . \qquad (8)$$

A non-zero value of the "coupling constant" α allows the width of the valley to vary over the saddle, and by doing so couples the two degrees of freedom. Fig.2 shows such a potential surface for the Eckard barrier for the special case of $\alpha = 0.1$ and $\hbar\sqrt{C/m_y}/V_o = 0.1$ (i.e. the frequency of the oscillator in the asymptotic region is one tenth of the barrier height).

Most of the calculations were carried out with a Gaussian barrier and the numerical values of the parameters were chosen so as to correspond to a typical fission case:

$$\begin{aligned} m_x &= 500\ \text{MeV}^{-1} & V_o &= 7\ \text{MeV} & a &= 0.185 \\ m_y &= 4.7\ \text{MeV}^{-1} & C &= 5.1\ \text{MeV} \ . \end{aligned} \qquad (9)$$

This choice of m_y and C gives a frequency of about 1 MeV, typical of, say, a gamma vibrational mode. The coordinates x

and y are dimensionless and correspond, for instance, to the deformation parameters ε_2 and ε_4 .

In the asymptotic region ($|x|\to\infty$) the two degrees of freedom decouple and the system finds itself with a certain probability in a definite quantum state in the transverse harmonic degree of freedom. Our goal is, if initially (i.e. for $x\to -\infty$) the system is in a state with a quantum number n_μ (for the transversal degree of freedom), to calculate the probability $T_{\nu\mu}$ to find the system after the tunneling (i.e. for $x\to +\infty$) in a quantum state n_ν. Of course, there is also a probability $R_{\mu'\mu}$ for the system to be reflected and to find itself at the end in a state μ' at $x\to -\infty$.

3. Quantum Mechanical Solution

In this section we will describe a full quantum-mechanical solution of the scattering problem for a Hamiltonian of the form given in eq.(7). The coordinate dependence of the inertial parameters is neglected for the sake of simplicity. However, the method is not restricted to such cases. It can easily be extended for more general Hamiltonians.

The Schrödinger equation we wish to solve is

$$\left\{\frac{\partial^2}{\partial x^2} + \frac{m_x}{m_y}\frac{\partial^2}{\partial y^2} + \frac{2m_x}{\hbar^2}\left(E - V(x,y)\right)\right\}\Psi(x,y) = 0 \qquad (10)$$

We expand the wave function in terms of a complete set of orthogonal functions in the coordinate y (for example, harmonic oscillator functions):

$$\Psi(x,y) = \sum_n u_n(x)\,\varphi_n(y). \qquad (11)$$

Substituting eq.(11) in eq.(10), multiplying from the left by $\varphi_n^*(y)$, and integrating over y, we find

$$-\frac{\hbar^2}{2m_x}\frac{d^2}{dx^2}u_n(x) + \sum_{n'} K_{nn'}(x)\cdot u_{n'}(x) = E\,u_n(x) \qquad (12)$$

with

$$K_{nn'}(x) = \int_{-\infty}^{+\infty}\varphi_n^*(y)\left\{-\frac{\hbar^2}{2m_y}\frac{d^2}{dy^2} + V(x,y)\right\}\varphi_{n'}(y). \qquad (13)$$

Eq.(12) are coupled channel equations which have to be solved with proper boundary conditions. In the

asymptotic region ($x \to \pm\infty$) there is no coupling, and the potential may be written as

$$H^{(\pm)} = -\frac{\hbar}{2m_x}\frac{\partial^2}{\partial x^2} + H_y^{(\pm)} . \qquad (14)$$

The eigenstates $\varphi^{(\pm)}(y)$ define the ingoing and outcoming channels

$$H_y^{(-)}\varphi_\mu^{(-)}(y) = \varepsilon_\mu \varphi_\mu^{(-)}(y) \; ; \quad H_y^{(+)}\varphi_\nu^{(+)}(y) = \varepsilon_\nu \varphi_\nu^{(+)}(y) \qquad (15)$$

In the following we use the indices $\nu, \nu', \ldots$ for the channels at $x \to +\infty$ and the indices $\mu, \mu', \ldots$ for the channels at $x \to -\infty$.

Let us express the asymptotic eigenstates $\varphi_\mu^{(-)}, \varphi_\nu^{(+)}$ in the basis $\varphi_n(y)$:

$$\varphi_\mu^{(-)} = \sum_n d_{n\mu}^{(-)} \varphi_n \; ; \quad \varphi_\nu^{(+)} = \sum_n d_{n\nu}^{(+)} \varphi_n \qquad 16)$$

The matrices $d^{(\pm)}$ are unitary. The wave function (11) is then given by

$$\Psi(x,y) = \begin{cases} \sum_{\nu n} d_{n\nu}^{(+)} \varphi_\nu^{(+)}(y) \cdot u_n(x) \\ \sum_{\mu n} d_{n\mu}^{(-)} \varphi_\mu^{(-)}(y) \cdot u_n(x) \; . \end{cases} \qquad (17)$$

The boundary conditions which the wave function $\Psi(x,y)$ has to fulfill are the following:

(i) for $x \to -\infty$ one shall have in all open channels ($\varepsilon_\mu < E$) only outgoing waves, except in the channel μ_o

where one has also an incoming wave with amplitude 1. In the closed channels ($\varepsilon_\mu > E$) there shall be only exponentially decreasing waves;

(ii) for $x \longrightarrow +\infty$ one shall have in the open channels only outgoing waves and in the closed channels only exponentially decreasing waves.

To assure that there are only outgoing waves for $x \longrightarrow +\infty$, one integrates numerically the coupled equations (12) starting from $x = +\infty$ with an outgoing wave in some channel ν. If the channel is closed, one starts with an exponentially decreasing wave (instead of an outgoing wave). Let $\bar{\Phi}_\nu(x,y)$ be the solution of this integration. For $x \longrightarrow +\infty$ it is given by

$$\bar{\Phi}_\nu(x,y) \underset{x\to+\infty}{=} \varphi_\nu^{(+)}(y) \cdot e^{ik_\nu x} \tag{18}$$

with $k_\nu = \sqrt{\frac{2m_x}{\hbar^2}(E-\varepsilon_\nu)}$ for the open channels ($\varepsilon_\nu < E$) and

$k_\nu = i\sqrt{\frac{2m_x}{\hbar^2}(\varepsilon_\nu - E)}$ for the closed channels ($\varepsilon_\nu > E$).

For the numerical integration, the system of second-order differential equations (12) is transformed into a system of first-order differential equations by introducing the derivations $v_n(x)$:

$$\begin{aligned} \frac{d}{dx} u_n(x) &= v_n(x) \\ \frac{d}{dx} v_n(x) &= \frac{2m_x}{\hbar^2} \sum_{n'} K_{nn'}(x)\, u_{n'}(x) - \frac{2m_x E}{\hbar^2} u_n(x) . \end{aligned} \tag{19}$$

The integration is performed by solving the system (19) starting at $x = +\infty$ with

$$u_n^{(\nu)}(+\infty) = d_{n\nu}^{(+)} e^{ik_\nu x} \quad ; \quad v_n^{(\nu)}(x) = ik_\nu d_{n\nu}^{(+)} e^{ik_\nu x} . \tag{20}$$

At $x = -\infty$, the wave function can be written in the form:

$$\Phi_\nu(x,y) \underset{x\to-\infty}{=} \sum_\mu \left(a_{\mu\nu} e^{ik_\mu x} + b_{\mu\nu} e^{-ik_\mu x}\right) \varphi_\mu^{(-)}(y). \tag{21}$$

The coefficients $a_{\mu\nu}$, $b_{\mu\nu}$ are evaluated from the values of $u_n^{(\nu)}(x)$ and $v_n^{(\nu)}(x)$ for $x \to -\infty$ found by integrating numerically eq. (19).

Using the unitarity relations for the coefficients $d_{n\mu}^{(-)}$ one finds:

$$a_{\mu\nu} = \lim_{x\to-\infty} \frac{1}{2} e^{-ik_\mu x} \sum_n d_{n\mu}^{(-)*} \left(u_n^{(\nu)}(x) + \frac{1}{ik_\nu} v_n^{(\nu)}(x)\right) \tag{22}$$

$$b_{\mu\nu} = \lim_{x\to-\infty} \frac{1}{2} e^{ik_\mu x} \sum_n d_{n\mu}^{(-)*} \left(u_n^{(\nu)}(x) - \frac{1}{ik_\nu} v_n^{(\nu)}(x)\right) \tag{23}$$

The final solution $\Psi^{(\mu_0)}(x,y)$ with the proper boundary conditions is a linear superposition of the functions $\Phi_\nu(x,y)$

$$\Psi^{(\mu_0)} = \sum_\nu C_{\nu\mu_0} \Phi_\nu \tag{24}$$

where the coefficients $C_{\nu\mu_0}$ are determined from the boundary conditions

$$\begin{aligned} &\text{(i)} \quad \Psi^{(\mu_0)} \quad (x \to +\infty) \quad = \text{only outgoing waves} \\ &\text{(ii)} \quad \Psi^{(\mu_0)} \quad (x \to -\infty) \quad = e^{i(k_{\mu_0} x)} \cdot \varphi_{\mu_0}^{(-)}(y) + \text{out-} \\ &\qquad\qquad\qquad\qquad\qquad\qquad\qquad\qquad\qquad\qquad \text{going waves.} \end{aligned} \tag{25}$$

The condition (i) is fulfilled by construction (all the Φ_ν fulfill it); condition (ii) determines $c_{\mu\nu_0}$:

$$\sum_\mu a_{\mu\nu} c_{\nu\mu_0} = \delta_{\mu\mu_0} . \tag{26}$$

That is, one finds $c_{\nu\mu_0}$ by a complex matrix inversion

$$c_{\nu\mu_0} = \left(a^{-1} \right)_{\nu\mu_0} . \tag{27}$$

Once $\underline{\Psi}^{(\mu_0)}$ is known, one can evaluate with eqs.(24), (21), and (18) the transmission probability

$$T_{\nu\leftarrow\mu_0} = |c_{\nu\mu_0}|^2 = |(a^{-1})_{\nu\mu_0}|^2 \tag{28}$$

and the reflection probability

$$R_{\mu\leftarrow\mu_0} = |(b\cdot c)_{\mu\mu_0}|^2 = |(b\cdot a^{-1})_{\mu\mu_0}|^2 . \tag{29}$$

There are, however, some restrictions to the method just described to solve the exact coupled channel eqs.(12), which limit the usefulness of this method for practical calculations:

(i) For realistic energy surfaces many channels must be included in order to obtain convergence in the expansion (11). This increases tremendously the amount of computer time.

(ii) The exponentially growing solutions within the closed channels present a serious numerical problem. Practical calculations are only possible if the closed channels can more or less be neglected. In the present calculations at most two closed channels were included. If many closed channels are important, one has to apply more sophisticated

methods. One way to avoid these difficulties is to expand the wave function for the closed channels by bound state wave functions to make sure that they contain no exponentially increasing components.

Another way is to choose different complete sets for different x-values. As an example, let us consider the potential (8):

$$V(x,y) = V(x) + \frac{1}{2} C(x) \cdot y^2 \ . \tag{30}$$

It is an harmonic oscillator potential for each value of x. The coupling is introduced by the x-dependence of the oscillator length

$$b(x) = \left(\frac{\hbar^2}{m_y \cdot C(x)} \right)^{1/4} \tag{31a}$$

and the oscillator frequency

$$\omega(x) = \left(C(x) / m_y \right)^{1/2} \tag{31.b}$$

Instead of eq.(11) we now make the ansatz

$$\Psi(x,y) = \sum_n u_n(x) \cdot \frac{1}{\sqrt{b(x)}} h_n\left(\frac{y}{b(x)}\right) \tag{32}$$

where $\frac{1}{\sqrt{b}} \cdot h(y/b)$ are properly normalized oscillator wave functions with the oscillator length $b(x)$.

Instead of eq.(12), one now finds

$$\left(-\frac{\hbar^2}{2m_x} \frac{d^2}{dx^2} + V(x) + \hbar\,\omega(x)\left(n+\tfrac{1}{2}\right) - E \right) u_n(x)$$
$$= \sum_{n'} \left(L_{nn'}(x) \frac{d}{dx} u_{n'}(x) + \tilde{K}_{nn'}(x) \cdot u_{n'}(x) \right) \tag{33}$$

with

$$L_{nn'}(x) = 2\cdot\int_{-\infty}^{+\infty} dy\ \frac{1}{\sqrt{b(x)}}\cdot h_n^*\left(\frac{y}{b(x)}\right)\cdot\left[\frac{\partial}{\partial x}\left(\frac{1}{\sqrt{b(x)}}\cdot h_{n'}\left(\frac{y}{b(x)}\right)\right)\right] \quad (34)$$

$$\tilde{K}_{nn'}(x) = \int_{-\infty}^{+\infty} dy\ \frac{1}{\sqrt{b(x)}}\ h_n^*\left(\frac{y}{b(x)}\right)\left[\frac{\partial^2}{\partial x^2}\left(\frac{1}{\sqrt{b(x)}}\cdot h_{n'}\left(\frac{y}{b(x)}\right)\right)\right]. \quad (35)$$

Using the properties of the harmonic oscillator wave functions h_n, one finally obtains

$$L_{nn'} = -\frac{b'}{b}\left\{\delta_{nn'} + 2\langle n|z\frac{\partial}{\partial z}|n'\rangle\right\} \quad (36)$$

$$\tilde{K}_{nn'} = \left(\frac{b'}{b}\right)^2\left\{\frac{3}{4}\delta_{nn'} + 3\langle n|z\frac{\partial}{\partial z}|n'\rangle + \langle n|z^2\frac{\partial^2}{\partial z^2}|n'\rangle\right\}$$
$$-\frac{2b''}{b}\left\{\delta_{nn'} + 2\langle n|z\frac{\partial}{\partial z}|n'\rangle\right\}. \quad (37)$$

Eq.(33) is then solved as described previously.

From eq.(34) one obtains a zero'th approximation by neglecting the coupling terms L and $\tilde{K}$. In that case one has no mixing of the channels. For each channel one has a one-dimensional barrier penetration problem. However, the form of the barrier is now modified by the x-dependent oscillator energy $\hbar\omega(x)\cdot(n+1/2)$, as shown in fig. 3. The corresponding wave functions are usually called "adiabatic" states. In ref. 19 the adiabatic states were calculated by a one-dimensional WKB-approximation and the coupling treated in Born-approximation. It has also

been pointed out by Maruhn and Greiner/20/ that in replacing the multidimensional barrier by the motion along a one-dimensional fission path, one has at least to correct for the change of the zero-point energy along that path.

For our simple model described in chapter 2 we took into account as many channels as were necessary to obtain convergence. For coupling constants $|\alpha| < 0.15$ at most two closed channels had to be included. Up to this value of the coupling constant the method previously described provides an exact quantum mechanical solution to which one can compare the semiclassical approximation, which we describe in the next section.

4. The semiclassical theory

4.1. THE INTEGRAL REPRESENTATION OF THE S-MATRIX

As mentioned in the introduction, we assume that there exists a classical Hamilton function (eq.(2)) which describes the same system as the quantum-mechanical Hamilton operator (eq.(1)). For this case W.H. Miller /14-16/and R.A. Marcus /17,18/ have derived semiclassical approximations for the quantum-mechanical S-matrix.

In this section we apply the method developed by Marcus /17,18/ to the two-dimensional barrier penetration problem defined in section 2. The Hamilton function depends on the fission coordinate x, the corresponding momentum p and on the "internal" degree of freedom y with its canonically conjugate momentum p_y. The correspondence between the quantum-mechanical problem, where the y-motion is quantized, and the classical theory is most easily achieved if an action variable J and an angle variable w[13] is used for this degree of freedom.

For our model (Chap.2) they are given by

$$J = \frac{\pi}{\omega(x)} \left(C(x) \cdot y^2 + \frac{p_y^2}{m_y} \right) \tag{38}$$

$$w = -\frac{1}{2\pi} \operatorname{Arctg} \left(p_y / (\omega(x) \cdot m_y \cdot y) \right) .$$

From the classical Hamilton function in these coordinates $H(p, J, x, w)$ the quantum-mechanical Hamiltonian is obtained by the substitutions

$$J \rightarrow \frac{\hbar}{i} \frac{\partial}{\partial w} + 2\pi\hbar\xi \quad , \qquad p \rightarrow \frac{\hbar}{i} \frac{\partial}{\partial x} \quad . \tag{39}$$

The constant ξ describes the difference between the classical action variable J and the quantum-mechanical operator $\frac{\hbar}{i}\frac{\partial}{\partial w}$. It is different for different types of internal degrees of freedom/21/. For an harmonic oscillator (present case) it has the value $^1/_2$ in the WKB limit.

In the asymptotic region there is no coupling between the two degrees of freedom. The internal state is described by the quantum number n, and for the x-motion one has a plane wave with the wave number k_n. The wave function is therefore given by

$$\varphi^{o(\pm)}_{nE}(x,w) = e^{i(\pm k_n \cdot x + 2\pi n \cdot w)} . \qquad (40)$$

The total energy is fixed and has the value

$$E = \frac{\hbar^2 k_n^2}{2m_x} + \varepsilon_n \qquad (41)$$

where $\varepsilon_n = \hbar\omega_0(n+1/2)$ is the internal energy.

Following Dirac /22/, one now makes the WKB ansatz for the wave function

$$\Psi = A \cdot e^{\frac{i}{\hbar}W - 2\pi i w \cdot 1/2} \qquad (42)$$

and substitutes this ansatz into the Schrödinger equation. Expanding in terms of $\hbar$ one obtains for the lowest order in $\hbar$ the Hamilton-Jacobi /13/ equation

$$H\left(\frac{\partial W}{\partial x}, \frac{\partial W}{\partial w}, x, w\right) = E \qquad (43)$$

which allows a determination of the action W.

To the next order in $\hbar$ one obtains a continuity equation for the amplitude A:

$$\frac{\partial}{\partial w}\left(A^2 \cdot \dot{w}\right) + \frac{\partial}{\partial x}\left(A^2 \cdot \dot{x}\right) = 0 \qquad (44)$$

where the dots indicate time derivatives and are given by

$$\dot{x} = \frac{\partial H}{\partial p} \qquad \dot{w} = \frac{\partial H}{\partial J} \quad . \qquad (45)$$

From classical mechanics/13/one knows how to solve eq. (43). One has to find the solutions of the classical equations of motion (45) (classical trajectories). The time derivative of Hamiltons characteristic function W is

$$\frac{d}{dt} W = p \cdot \dot{x} + J \cdot \dot{w} \quad . \qquad (46)$$

Integrating eq.(46) with the proper initial condition that for $t < t_o$ (t_o being a time before any interaction takes place) one has an incoming wave in the channel μ (see eq.(40)), one obtains

$$W = \int_{t_o}^{t} (p \cdot \dot{x} + J\dot{w})\, dt' + \hbar\left(k_{n_\mu} x^o + 2\pi w^o (n_\mu + \tfrac{1}{2})\right) \qquad (47)$$

where $x^o = x(t_o)$ and $w^o = w(t_o)$. The integrals are line integrals, the integration being performed along the classical trajectories which the system traces. "Classical" means that the trajectories are solutions of the classical equations of motion(44). It is not necessary, however, that these be real solutions. In fact there are classically forbidden

regions which cannot be reached by real trajectories. The barrier penetration is an example of such a case. In order to find trajectories reaching these regions, one has to use complex trajectories, as will be discussed in the next section. Here we assume that we have found such solutions and discuss how to find an expression for the wave function which fulfills the proper boundary conditions.

Eq.(44) is a continuity equation. Integrating it over a tube spanned by classical paths starting at a point x^o ($A(x^o) = 1$) we find

$$A(x) = \left(\frac{v^o}{v} \Big/ \frac{dw}{dw^o} \right)^{1/2} \tag{48}$$

with $v^o = \dot{x}(t_o)$.

In the asymptotic region we therefore have the wave function

$$\psi(x,w) \underset{x\to+\infty}{=} \left(\frac{v^o}{v} \Big/ \frac{dw}{dw^o} \right)^{1/2} \exp\left(\frac{i}{\hbar} W - i\pi w \right). \tag{49}$$

For negative x-values we have a superposition of the incoming and the reflected wave

$$\psi(x,w) \underset{x\to-\infty}{=} \varphi^{o\,(+)}_{n_\mu E} + \left(\frac{v^o}{v} \Big/ \frac{dw}{dw^o} \right)^{1/2} \exp\left(\frac{i}{\hbar} W - i\pi w + i\frac{\pi}{2} \right). \tag{50}$$

For the reflected wave one has to increase the phase by $\pi/2$ when p changes from positive to negative (i.e. when x goes through a turning point) /21/.

Since we now have constructed a semiclassical wave function, the next step is to obtain an expression for the S-matrix. The matrix elements of the S-matrix can be found from the asymptotic expressions 49 and 50 and are given by

$$\Psi \underset{x\to\infty}{=} -\sum_{\nu} S_{\nu\mu}^{tr} \sqrt{\frac{v^{(\mu)}}{v^{(\nu)}}}\, \varphi^{o\,(+)}_{n_\nu E} \tag{51}$$

and

$$\Psi \underset{x\to-\infty}{=} \varphi^{o\,(+)}_{n_\mu E} - \sum_{\nu} S_{\nu\mu}^{refl} \sqrt{\frac{v^{(\mu)}}{v^{(\nu)}}}\, \varphi^{o\,(-)}_{n_\nu E} \tag{52}$$

Once the S-matrix is known, the transition probabilities for the system from an initial state μ to a final state ν are given by

$$P_{\nu\leftarrow\mu} = |S_{\nu\mu}|^2 \tag{53}$$

Comparing eqs.(51) with (49) and (52) with (50), we find after multiplying both sides by $\exp(-2\pi i n_\nu w)$ and integrating over the angle w that

$$S_{\nu\mu} = \lim_{t\to\infty} \int_{-1/2}^{1/2} dw \left(\frac{v^{\nu}}{v(t)} \Big/ \frac{dw}{dw^{o}}\right)^{1/2} e^{\frac{i}{\hbar}\Delta(w)} \tag{54}$$

with

$$\Delta = -\int_{t_o}^{t} (x\cdot\dot{p} + w\cdot\dot{J})\,dt' + 2\pi\hbar w\,(n(t)-n_\nu) + x\,(p(t)\mp\hbar k_\nu) \tag{55}$$

where the upper sign holds for transmitted and the lower sign for reflected waves. For the latter case an additional phase of $-\pi/2$ has to be added to Δ .

The final angle w is a function of the initial angle w°. Changing the integration variable from w to w° one obtains

$$S_{\nu\mu} = \lim_{t\to\infty} \int_{-1/2}^{1/2} dw^\circ \left(\frac{v^{(\nu)}}{v(t)} \cdot \frac{dw}{dw^\circ}\right)^{1/2} e^{\frac{i}{\hbar}\Delta(w^\circ)} \quad . \tag{56}$$

The functions $n(t) = J(t)/2\pi\hbar$ and $p(t)$ are time independent for large t-values. However, the asymptotic values n_f and p_f depend on the initial angle w°. Eq.(56) is the so-called integral representation of the S-matrix derived first by R.A. Marcus and coworkers/17,18/. It has been used recently in an exactly soluble model/23/and turned out to be very useful . Within this paper, however, we go one step further and apply the saddle-point approximation to the integral in eq. (56).

4.2. THE SADDLE-POINT APPROXIMATIONS

In deriving the semiclassical S-matrix (56), we used the WKB ansatz for the wave function, which decomposes it into an amplitude and a rapidly oscillating phase. Both were calculated only for small values of $\hbar$. Therefore it seems consistent to apply the same argument once more and to use a saddle-point approximation for the integral (56). This approximation uses the fact that the phase $e^{i\Delta/\hbar}$ is rapidly oscillating and that there will be contributions to the integral (56) only from values w° , for which the phase

becomes stationary, (saddle points)

$$\frac{d\Delta}{dw^\circ} = 0 \quad . \tag{57}$$

There exist several approximations to an integral of the type (56) which take into account only the values and certain derivatives of the integrand at the points of stationary phase. Three of them (the so-called primitive semiclassical approximation, the Airy- and the Bessel approximation) are considered in the appendix.

In order to find the saddle points, one has to find the solutions of eq.(57). For this purpose we go back to the representation (55) and note that from (47) one has

$$\begin{aligned}\Delta(w) = W(w,x) - 2\pi\hbar\, w\cdot n_\nu - 2\pi\hbar\, w^\circ(n_\mu+\tfrac{1}{2}) \\ - \hbar\, x\cdot k_{n_\nu} - \hbar\, x^\circ k_{n_\mu}\end{aligned} \tag{58}$$

and for $t \longrightarrow +\infty$

$$\frac{d\Delta}{dw} = \frac{\partial W}{\partial w} - 2\pi\hbar\, n_\nu = J - 2\pi\hbar\, n_\nu \quad . \tag{59}$$

The points of stationary phase are therefore given by the condition

$$n_f(w^\circ) = \lim_{t\to\infty} J(t)/2\pi\hbar = n_\nu \quad . \tag{60}$$

To find such stationary solutions, one has to solve the classical equations of motion

$$\begin{aligned}\dot{x} &= \frac{p}{m_x} \quad ; \qquad \dot{p} = -\frac{\partial}{\partial x} V(x,y) \\ \dot{y} &= \frac{p_y}{m_y} \quad ; \qquad \dot{p}_y = -\frac{\partial}{\partial y} V(x,y)\end{aligned} \tag{61}$$

with the initial values X^o (large and negative), p^o (given by energy conservation), n_μ and w^o, and to calculate the final "action" variable $n_f(w^o)$ (quantum number function).[+] The stationary points of the phase are the points w^o for which the quantum number function has the real integer value n_ν. Usually eq. (60) has several solutions, which corresponds to different saddle points.

The model considered in the present paper has a symmetry. The Hamiltonian does not change when changing y to -y. It is therefore sufficient to take into account only the range $0 \leq w^o \leq 1/2$. If w^o is a solution of eq.(60), then $w^o + 1/2$ is also a solution, but from (54) and (56) one has

$$\Delta(w^o + 1/2) = \Delta(w^o) - \pi (n_\nu - n_\mu) \quad . \tag{62}$$

For odd values of $n_\mu - n_\nu$ the matrix element $S_{\nu\mu}$ vanishes (parity selection rule). For even values of $n_\mu - n_\nu$ one needs to take into account only the saddle points in the interval $0 \leq w^o \leq 1/2$ and then multiply the resulting

---

[+] Here we have (eq.(61)) written the equations of motions in cartesian coordinates y, p_y. Obviously they have to be transformed into the action angle variables in the asymptotic region in order to impose the right boundary conditions. For our simple model we could have solved the equations of motion in action angle variables as well. This, however, often introduces numerical difficulties.

S-matrix elements by a factor 2.

For our model one has always two saddle points in this interval : ω_1 and ω_2 . The corresponding angles are $\phi_i = 2\pi\omega_i$. The phases Δ_i at these points are (eq.(55))

$$\Delta_i(n_\nu, n_\mu) = -\int_{-\infty}^{+\infty} (x\dot{p} + \omega\dot{J})\,dt' \qquad (i=1,2) \tag{63}$$

and (with (59))

$$\left.\frac{d^2\Delta}{d\omega^{\circ 2}}\right|_{\omega^\circ=\omega_i} = 2\pi\hbar \left(\frac{dn_f}{d\omega^\circ}\right)_{\omega^\circ=\omega_i} \cdot \left(\frac{d\omega}{d\omega^\circ}\right)_{\omega^\circ=\omega_i} . \tag{64}$$

We therefore find from the appendix and eqs.(63) and (64) that in the primitive semiclassical approximation the S-matrix is given by

$$S_{\nu\mu} = \sum_{i=1}^{2} \frac{1}{\sqrt{\left.\frac{dn_f}{d\omega^\circ}\right|_{\omega^\circ=\omega_i}}}\, e^{i\Delta_i(n_\nu,n_\mu)} \cdot \left(1 + (-)^{n_\mu+n_\nu}\right) \tag{65}$$

$$= \frac{\left(1+(-)^{n_\mu+n_\nu}\right)}{2}\left\{\sqrt{p_1}\, e^{i\Delta_1} + \sqrt{p_2}\, e^{i\Delta_2}\right\}$$

where $$p_i = \frac{2}{\sqrt{\left.\frac{dn_f}{d\omega^\circ}\right|_{\omega^\circ=\omega_i}}} \qquad (i = 1,2) . \tag{66}$$

$|p_i|$ are the classical probabilities, and the purely classical S-matrix element would be $\sqrt{|p_1|} + \sqrt{|p_2|}$. The semiclassical approximation, however, takes into account the phases

for the stationary trajectories and, for forbidden transitions, allows the p_i's to become complex.

As discussed in the appendix, one has to consider very carefully whether a stationary solution has to be included in the sum (65). For classically forbidden processes only one of them has to be included. For the Airy- and the Bessel-uniform approximation it is not necessary to make such distinction. For the present tunneling problem we used the Bessel uniform approximation. With $K = |n_\mu - n_\nu|$ one finds for the S-matrix element (eq.(A.8))

$$S_{\nu\mu} = \frac{1}{2}(1+(-)^K)\left(\frac{2\pi\xi}{\sqrt{1-\left(\frac{K}{2\xi}\right)^2}}\right)^{1/2}\left\{\sqrt{1-\left(\frac{K}{2\xi}\right)^2}\left(\sqrt{p_1}+\sqrt{p_2}\right)J_{\frac{K}{2}}(\xi)\right. \tag{67}$$
$$\left. + i\left(\sqrt{p_1}-\sqrt{p_2}\right)J'_{\frac{K}{2}}(\xi)\right\}$$

where ξ is implicitly given by

$$\frac{1}{2}(\Delta_2-\Delta_1) = \xi\sqrt{1-\left(\frac{K}{2\xi}\right)^2} + i\frac{K}{2}\,\mathrm{Ln}\left(\frac{K}{2\xi}+i\sqrt{1-\left(\frac{K}{2\xi}\right)^2}\right). \tag{68}$$

4.3. CLASSICALLY FORBIDDEN PROCESSES

In section 4.1 we considered a WKB-ansatz (42) for the wave function. The phase W was determined by the classical Hamilton-Jacobi equation (43). This equation was then solved by the method of characteristics by which one introduces a time parameter and trajectories obeying the classical equations of motion. As long as one regards

only real trajectories (i.e. real coordinates, momenta and times), it is obvious that there are certain regions of the phase space which cannot be reached (classically forbidden regions).

For the problem considered here there are two types of forbidden regions:

(i) For the reflected trajectories there is only a finite time during which the system feels a coupling between the two degrees of freedom x and y. As long as the coupling strength (α) is finite, there exist usually quantum numbers n_f which cannot be reached by real trajectories, i.e. for fixed n_i the equation

$$n_f\ (w^o) \;=\; n \tag{69}$$

does not have for all values of n real solutions w^o, even if they are energetically allowed. However, allowing complex initial values w^o it is possible to find such trajectories with a real time path. Complex initial conditions lead to a complex phase Δ, i.e. to an exponentially decreasing probability (see eq.(65)). For real time paths, also w^{o*} is a solution of (60), but as discussed in ref. 24, only the saddle point in the complex w^o-plane giving an exponentially decreasing contribution should be taken into account within the primitive semiclassical approach (eq.(65)).

Since the initial "phase" w^o is not physically ob-

servable, one has no difficulties in allowing it to be complex. It is evident that one does not need complex trajectories, if the integral representation (56) for the S-matrix is used. For this case, using the analytic properties of the integrand, it is sufficient to integrate along the real interval $0 \leq w^0 \leq 1$.

(ii) The situation is completely different for the tunneling situation ($E < V$). As long as one starts with real x- and p-values and uses real time increments only, it is not possible to find trajectories which end up, for $t \rightarrow \infty$, at the other side of the barrier (even allowing complex initial angles w^0). That means that, for such trajectories, the wave function vanishes on the right-hand side of the barrier. To get there a non-vanishing wave function, one has to allow for complex time paths. This has been studied in detail by W.H. Miller et al. (ref. 15) in the analytically soluble one-dimensional example of a symmetrical Eckard potential barrier. It is shown there that for certain time paths im the complex time plane one obtains a reflected wave, and for other paths one gets tunneling. For this analytically soluble model one knows the analytic structure of the function Δ and one therefore knows in which sheet of this multivalued function one has to carry out the analytical continuation of the classical S-matrix. For the two-dimensional problem considered in the present paper one does not know the analytical structure and therefore it is not so straight-forward

to find the tunneling trajectories which contribute to the S-matrix. For our problem, one could always find two such tunneling trajectories. Since the time increments are no longer real, ω_1^{o*} now differs from ω_1^{o}. Fig. 4 shows for a particular case the quantum number n_f as a function of the initial angle $\phi_o = 2\pi\omega^o$. One observes that the quantum number function is rather "flat" and therefore the Bessel uniform approximation for the S-matrix was used.

5. Results and Comparison

We shall now present numerical results for the tunneling problem described by the model Hamiltonian (eq.8) using the different methods discussed in the last two sections.

Fig.4 shows in its upper part the shape of the Gaussian barrier (parameters are those of eq.9) together with the adiabatic translational energies in the x-direction for the three y-vibrational channels n=o, n=2, n=4. The total energy is chosen to be E_{tot}= 6 MeV and the coupling strength is α=o.1. That means we are dealing with a typical subfission barrier with ~ 5.5 MeV of excitation and ~1.5 MeV below the classical barrier threshold. Higher n-channels are obviously closed, and odd n-channels are not coupled for parity reasons.

The lower part of fig.5 shows the square of the wavefunction for an incident wave from the left in channel μ=2 (i.e. $|u_2^{(\nu)}(x)|^2$). These results were obtained using the exact coupled channel quantum mechanical code described in section 3. In the coupled channel code, three open and one closed channel were included. Taking into account the fourth (closed channel) changes the results only in the fourth significant figure. We note the standing wave in the channel μ=2 on the left side of the barrier, as most of the flux is elastically reflected. About 10^{-5} is inelastically reflected in channel μ=4 and 10^{-8} in channel μ=o. To the right of the barrier ν=o, 2 and 4 waves are transmitted at the 10^{-10}, 10^{-15} and 10^{-24} probability levels respectively.

Fig.6 shows how the penetrabilities $P_{\nu\mu}$ change with the coupling strength α between α =-o.15 and α=+o.15. These values of α correspond to a not too strong coupling between the two degrees of freedom. Larger values of α were not considered, since in order to expand the wavefunction eq.11, many more channels have to be included. From fig.6 we find that there is a vibrational "cooling" effect on the passage through the barrier, with ν=0 transmitted waves dominating regardless of the vibrational state incident on the barrier. Only in the case of very close to zero, (constant valley width), will this cooling not occur. The reason for this effect is, that the tunneling probability in a channel ν with low vibrational quantum number has more energy available for the translational motion, which favours tunneling. As soon as the system - through the coupling of the two degrees of freedom - has moved into a vibration with lower vibrational energy its tunneling probability is much higher and therefore transitions to lower ν-values are favoured. Obviously this is not a real cooling in the statistical sense. The transition is completely reversible and the transition probability $P_{\nu\mu}$ from the channel μ to the channel ν is equal to the transition probability $P_{\mu\nu}$.

In the following we first discuss diagonal transitions. An obvious approximation to be tested by the coupled channel solution is the so-called vibrationally adiabatic approximation (QM_{ad}), where one assumes that during the fission process the system

always stays in the same oscillator state μ. We only allow the wave function in the y-direction to adjust adiabatically as the width of the valley changes along the path. In this case one neglects the right-hand side of eq. 33. Table 1 shows the diagonal transition probabilities $P_{\mu\mu}$ for the no-coupling case ($\alpha = 0$) obtained with the exact quantum-mechanical code (QM) and for the vibrationally adiabatic approximation (QM_{ad}). Since for the model studied here the inertial tensor is coordinate-independent and diagonal, the one-dimensional WKB approximation (eq.3) and the least-action path method (eq.5) give the same result (also shown in table 1) and are independent of α.

For $\alpha = 0.1$ one finds that the QM_{ad} calculation is quite good, considerably better than the WKB result. The main reason why the WKB result and the least-action path method give larger penetrability values is because they neglect the change of the zero-point energy in the y-motion, which increases around the barrier for positive α-values (the valley becomes narrower at the top of the barrier), leaving less energy available in the fission degree of freedom to penetrate the barrier.

Neither the WKB nor the least-action path method permit the calculation of off-diagonal transitions (that is, cases for which the final quantum number is different from the initial quantum number). This, however, is no difficulty in the semi-classical approach described in section 3. Table 2

shows a comparison between the uniform semi-classical approximation USCA (eq.(67)) and the exact QM calculations. For $\alpha = 0$ the USCA results are identical to the WKB results shown in table 1 (only the diagonal transitions are non-vanishing for $\alpha = 0$). In fig. 6 the USCA results are shown by dots. The agreement between these USCA calculations and the exact quantum-mechanical coupled channel calculations is very good, even though the model considered here is highly non-classical.

Up to now we have discussed a Gaussian barrier. A barrier of the shape $f(z) = \cosh^{-2}(z)$ in eq.(8) (Eckard-potential) can be treated analytically in the one-dimensional case. In the two-dimensional case this is no longer possible. However, in the so-called sudden limit the two-dimensional problem can be solved analytically. This limiting situation is obtained by letting m_y become very large and C very small so that $C \cdot m_y$ remains constant. In this case the system does not oscillate during the tunneling process. The details of the analytical solution are given in ref. 23, therefore we give only some results here.

In the following the parameters

$$m_x = 500 \text{ MeV}^{-1}; \quad V_o = 7 \text{ MeV}; \quad a = 0.120 \qquad (70)$$

were used.

The constants C and m_y are not relevant in the sudden limit. We take the initial quantum number to be $\mu_o = 4$ because in this case one has both excitation and de-excitation of the oscillator, and the total energy to be E = 3.5 MeV.

Fig. 7 shows the exact quantum-mechanical probabilities for tunneling $P^{trans}_{\nu\mu_0}$ and for reflection $P^{refl}_{\mu\mu_0}$ as a function of the coupling strength α. For $\alpha = 0$ the system remains in the oscillator state n = 4. With increasing α transitions to other oscillator states can take place. For the reflected waves the population of the different channels oscillates with increasing α. The corresponding semi-classical solution shows that there are always two trajectories which contribute to the S-matrix with an amplitude of the same order of magnitudes. This produces an interference. For the transmitted waves no such oscillations occur. The reason is that only one of the two classical trajectories contributes to the S-matrix. The other one has an amplitude which is smaller by several orders of magnitude.

For very small coupling constants the transition to states with higher n-quantum numbers are favoured because the matrix element which couples n with n + 2 is larger than the one which couples n to n - 2. But with increasing α the states with lower n-values are favoured because they see a lower barrier as discussed before.

Tables 3 and 4 show the actual values of the transmission and reflection probabilities for the case of $\alpha = 0.1$. The exact quantum-mechanical solutions are compared with the different semi-classical approximations discussed in section 4, namely the primitive semi-classical (eq.(65)), the Bessel (eq.(67)), and the Airy (eq.(A.4)) approximation

to the full integral (eq.(56)) which is given in the last column. The over-all agreement with the quantum-mechanical results is excellent.

6. Conclusion

In this paper we have investigated the tunneling through a two-dimensional fission barrier. A simple model was introduced and treated in several ways:

(i) An exact quantum-mechanical solution of the problem is possible by a coupled-channel calculation. This method is general enough to be extended to more complicated problems; however, difficulties arise in cases where too many closed channels have to be included in the calculation.

(ii) The application of the uniform semi-classical approximation developed by W.H. Miller /14-16/ and R.A. Marcus /17,18/ to the fission problem is proposed and investigated in this model. There are always two complex classical trajectories which fulfill the right boundary conditions. The corresponding amplitudes are added coherently to obtain the S-matrix. In the limit of a sudden collision one can study the behaviour of both trajectories analytically. The result is that for the reflected waves both trajectories have amplitudes of the same order of magnitudes. This produces an oscillating dependence of the reflection probabilities on the coupling strength α .

For the transmitted waves one of the amplitudes is usually much larger than the rest. Therefore in this case an interference structure is not found.

The agreement between the transition probabilities computed quantum-mechanically and semi-classically is very good. For diagonal transitions the most important effect resulting from the multi-dimensionality of the fission barrier seems to be the change of the barrier high due to the zero-point energy of the vibrational motion perpendicular to the fission path. If one takes this zero-point energy into account, the adiabatic approximation along a one-dimensional fission path seems to be satisfactory, at least as long as the coordinate dependence of the inertia tensor is ignored, and one is interested only in diagonal transitions.

The least-action path method /1/ is able to include a coordinate-dependent inertia tensor. It is, however, not able to include the effects of zero-point motion perpendicular to the fission path because it does not fulfill the right boundary conditions. Since it is very easy to include into the uniform semi-classical approximation also coordinate-dependent and non-diagonal inertial tensors, the latter seems to be an appropriate method to investigate multi-dimensional fission barriers, at least as long as the available total energy is not too close to the barrier top.

Up to now there has been no experimental data which

gives information about non-diagonal transition. Nevertheless, the USCA-method allows to calculate non-diagonal transition probabilities and the results agree well with the exact calculation.

We would like to express our gratitude to W.H. Miller for many helpful discussions. The research was largely supported by the U.S. Energy Research and Developement Administration. Two of us (P.R. and H.M.) wish to thank the Lawrence Berkeley Laboratory and in particular the Nuclear Science Group for the hospitality extended to them.

A p p e n d i x

We are interested in an approximate evaluation of the integral

$$I = \int_0^{\wedge} g(x)\, e^{i f(x)}\, dx \qquad (A.1)$$

where $\frac{df}{dx}$ is large over most of the interval (so that the integrand is rapidly oscillating) and has two saddles x_1 and x_2

a) The socalled "primitive" approximation is obtained when f is expanded up to quadratic terms around the points x_1 and x_2 separately. In this case I is decomposed into two parts and one gets

$$I \approx g_1 \sqrt{\frac{2\pi}{f_1''}}\, e^{i(f_1 + \pi/4)} + g_2 \sqrt{\frac{2\pi}{f_2''}}\, e^{i(f_2 + \pi/4)} \qquad (A.2)$$

with $f_i = f(x_i)$; $g_i = g(x_i)$

In the classically accessible case both saddle points are real. For the classical forbidden cases, however, the corresponding saddle points are complex. In applying this approximation one has to be therefore very careful and check the relative position and orientation of the saddles which may result that in some cases one has to take into account only one of them (see ref.24 and 23).

b) The approximation (A.2) is only good if the two saddle points x_1 and x_2 are well separated. When the two saddle

points x_1 and x_2 are close together one has to improve the prescription (A.2) and one way is to map the phase f onto a cubic in such a way that the stationary points of f and the cubic correspond[18,24,25)]

$$f(x) = \tfrac{1}{3}u^3 + \xi \cdot u + A = h(u) \qquad (A.3)$$

In this way one obtains the Airy-uniform approximation

$$I \approx \sqrt{2}\cdot\pi\, e^{i(f_1+f_2)/2} \cdot \left\{ \left(\frac{g_1}{\sqrt{f_1''}} + \frac{g_2}{\sqrt{-f_2''}} \right) \xi^{1/4} \cdot Ai(-\xi) + i \left(\frac{g_1}{\sqrt{f_1''}} - \frac{g_2}{\sqrt{-f_2''}} \right) \xi^{-1/4} \cdot Ai'(-\xi) \right\} \qquad (A.4)$$

with $\xi = \left[\frac{3}{4}(f_1 - f_2) \right]^{2/3}$

c) The mapping (A.3) is one of many possibilities. For the case of a functions f with the structure

$$f(x) = \tilde{f}(x) - 2\pi\varkappa x \qquad (A.5)$$

for constant $\varkappa$ and rather "flat" f, Stine and Marcus[26)] consider the mapping

$$f(x) = -\xi \cdot \cos(2y) + A + x \cdot y = h(y) \qquad (A.6)$$

from the interval $0 \leq x \leq 1$ onto the interval $-\pi \leq y \leq \pi$. The constants ξ and A are chosen so that the stationary phase points of f(x) in $0 \leq x \leq 1$ correspond to those of the new function h(y) in the new domain. This leads to

$$\begin{aligned} \tfrac{1}{2}(f_1 + f_2) &= A - \pi/4 \cdot \varkappa \\ \tfrac{1}{2}(f_1 - f_2) &= -\xi \sqrt{1 - \left(\frac{\varkappa}{2\xi}\right)^2} + i\,\frac{\varkappa}{2}\,\mathrm{Ln}\left(\frac{\varkappa}{2\xi} + i\sqrt{1 - \left(\frac{\varkappa}{2\xi}\right)^2} \right) \end{aligned} \qquad (A.7)$$

For integer values of this yields the so called Bessel uniform approximation

$$I \approx 2\pi \xi^{1/2} \left(1-\left(\frac{\kappa}{2\xi}\right)^2\right)^{-1/4} e^{i(f_1+f_2)/2} \cdot \left\{ \left(1-\left(\frac{\kappa}{2\xi}\right)^2\right)^{1/2} \left(\frac{g_1}{\sqrt{f_1''}}+\frac{g_2}{\sqrt{f_2''}}\right) J_{\frac{\kappa}{2}}(\xi) + i\left(\frac{g_1}{\sqrt{f_1''}}-\frac{g_2}{\sqrt{f_2''}}\right) J_{\frac{\kappa}{2}}'(\xi) \right\} \qquad (A.8)$$

The Bessel- and Airy-approximation is usually more complicated to apply than the primitive semiclassical approximation (eq.A.2), but they also are more general and have advantages in the case of complex saddle points. In ref. 23 the three methods are compared in detail in a simple model. In order to decide which one to use, one has to investigate the behaviour of the function f(x) in the integral (A.1). for complex saddle points (classically forbidden processes) this can be rather tedious, and in such cases it is often easier to evaluate the integral numcerically.

REFERENCES

1) M. Brack, J. Damgaard, A. Jensen, H.C. Pauli, V.M. Strutinski and C.Y. Wong, Rev. Mod. Phys. 44 (1972) 320

2) D.L. Hill and J.A. Wheeler, Phys. Rev. 89 (1953) 1102

3) B. Banerjee and D.M. Brink, Zeitschr. f. Phys. 258 (1973) 46

4) G. Holzwarth, Nucl. Phys. A207 (1973) 545

5) H. Flocard and D.Vautherin, Phys. Lett. 52B (1974) 399
B. Giraud and B. Grammaticos, Nucl. Phys. A255 (1975) 141

6) A. Kamlah, to be published

7) V.M. Strutinsky, Nucl. Phys. A95 (1967) 420; A122 (1968) 1

8) Y.M. Engel, D.M. Brink, K. Goeke, S.J. Krieger and D. Vautherin, Nucl.Phys. A249 (1975) 215

9) D.M. Brink, M.J. Giannoni and M. Veneroni, Nucl. Phys. A258 (1976) 237

10) S.G. Nilsson et al., Nucl. Phys. A131 (1969) 1

11) P.O. Fröman and N. Fröman, JWKB Approximation, Contribution to the Theory (North-Holland, Amsterdam, 1965)

12) B.S. Jeffreys, "The Asymptotic approximation method", review article in Quantum Theory I, ed.D.R. Bates (Academic Press, New York, 1961)

13) H. Goldstein, Classical Mechanics (Addison-Wesley, Reading, Mass., 1950)

14) W.H. Miller, J.Chem. Phys. 53 (1970) 1949;
53 (1970) 3578

15) W.H. Miller and T.F. George, J. Chem. Phys. 56 (1972) 5668;
T.F. George and W.H. Miller, J. Chem. Phys. 57 (1972) 2458;
J.D. Doll, T.F. George and W.H. Miller, J. Chem. Phys. 58 (1972) 1343

16) W.H. Miller, Adv. Chem. Phys. 25 (1974) 69; "The Classical S-Matrix in Molecular Collisions", in: Molecular Beams, ed. K.P. Lawley (Wiley, New York, 1975)

17) R.A. Marcus, Chem. Phys. Lett., 7 (1970) 525; J. Chem. Phys. 54 (1971) 3965

18) J.N.L. Connor and R.A. Marcus, J. Chem. Phys. 55 (1971) 5636

19) H. Hofmann, Nucl. Phys. A224 (1974) 116

20) J. Maruhn and W. Greiner, Phys. Lett. 44B (1973) 9

21) J.B. Keller, Ann. Phys. 4 (1958) 180

22) P.A.M. Dirac, The Principles of Quantum Mechanics,(Oxford U.Press, New York, 1958, 4th ed.)

23) H. Massmann, K.Möhring and P. Ring, J. Chem. Phys., in print

24) H. Massmann, Ph.D. thesis, LBL report 4316 (1975)

25) C. Chester, B. Friedman and F. Ursell, Proc. Cambridge Phil. Soc. 53 (1957) 599

26) J. R. Stine and R.A. Marcus, J. Chem. Phys. 59 (1973) 5145

Table 1

Comparison between the QM, QM_{ad} and WKB calculations of the diagonal transition probabilities $P_{\mu\mu}$

	$\alpha = 0$	$\alpha = 0.1$		
$\mu \to \mu$	QM	QM	QM_{ad}	WKB
$0 \to 0$	$1.67 \cdot 10^{-5}$	$1.40\ 10^{-5}$	$1.40\ 10^{-5}$	$1.60\ 10^{-5}$
$2 \to 2$	$5.48\ 10^{-13}$	$2.67\ 10^{-13}$	$2.42\ 10^{-13}$	$5.21\ 10^{-13}$
$4 \to 4$	$1.44\ 10^{-22}$	$4.66\ 10^{-23}$	$3.62\ 10^{-23}$	$1.34\ 10^{-22}$

Table 2

Comparison between the QM and the USCA transition probabilities $P_{\nu\mu}$

	$\alpha = 0.1$					$\alpha = 0.01$		
$\nu \leftrightarrow \mu$	$0 \leftrightarrow 0$	$0 \leftrightarrow 2$	$0 \leftrightarrow 4$	$2 \leftrightarrow 2$	$2 \leftrightarrow 4$	$0 \leftrightarrow 0$	$0 \leftrightarrow 2$	$0 \leftrightarrow 4$
QM	$1.4o\ 1o^{-5}$	$9.3o\ 1o^{-11}$	$1.o3\ 1o^{-16}$	$2.67\ 1o^{-13}$	$9.86\ 1o^{-19}$	$1.64\ 1o^{-5}$	$1.22\ 1o^{-12}$	$1.49\ 1o^{-2o}$
USCA	$1.44\ 1o^{-5}$	$9.49\ 1o^{-11}$	$o.97\ 1o^{-16}$	$2.52\ 1o^{-13}$	$9.15\ 1o^{-19}$	$1.56\ 1o^{-5}$	$1.3o\ 1o^{-12}$	$1.42\ 1o^{-2o}$

Table 3

Transition probabilities $P_{\nu\mu_o}$ (in units of 10^{-10}) in the sudden limit on an Eckard-shaped potential. The parameters are given in the text. $\mu_o = 4$

ν	QM	Pr.Semicl.	Bessel	Airy	Integral
0	2.8	1.9	1.9	1.9	3.0
2	2.6	2.3	2.3	2.3	2.8
4	2.2	2.0	2.0	2.0	2.3
6	1.7	1.5	1.5	1.5	1.7
8	1.2	1.0	1.1	1.1	1.2
10	0.77	0.68	0.69	0.69	0.76
12	0.45	0.42	0.43	0.43	0.47

Table 4

Reflection probabilities $P_{\mu\mu_o}$ for the sudden limit on an Eckard-shaped potential. The parameters are given in the text. $\mu_o = 4$

μ	QM	Pr.Semicl.	Bessel	Airy	Integral
0	0.041	0.048$^+$	0.039	0.040	0.053
2	0.32	0.35	0.32	0.35	0.31
4	0.016	0.019	0.015	0.016	0.016
6	0.14	0.11	0.14	0.14	0.13
8	0.22	0.001	0.23	0.23	0.23
10	0.15	0.079	0.15	0.15	0.16
12	0.065	0.33$^+$	0.068	0.069	0.069

$^+$ reflection is classically forbidden

Figure Captions

Fig. 1 Schematic representation of a fission barrier. Shown is the potential along the fission valley.

Fig. 2 Potential energy surface $V(x,y)/V_o$ (see eq.8) for the case of $f(z)=\cosh^{-2}(z)$. The parameters are $\alpha=0.1$ and $h(C/m_y)^{1/2}=0.1\cdot V_o$. x is measured in units of the barrier width a and y is measured in units of the oscillator length $b=(h^2/C\ m_y)^{1/4}$. Also drawn is the probability distribution for the harmonic oscillator wave function for the quantum states n=o and n=4.

Fig. 3 The effective barrier for the adiabatic states n=o,2,4. The lowest curve is the pure Gaussian barrier with the parameters of eq.(9). The other full lines include the x-dependent vibrational energy $\hbar\omega(x)\cdot(n+1/2)$. For the dashed lines the vibrational energy was taken to be constant $\hbar\omega_o\cdot(n+1/2)$. Shown also is the total energy of 6MeV used in the calculations to table 1 and 2 and fig.4,5 and 6.

Fig.4 Real and imaginary part of the quantum number function $n_\mu(\phi_o)$ versus the real part of ϕ_o ($\phi_o=2\pi\omega^o$). The various curves are labeled by the value of Imag (ϕ_o). The parameters are given in eq.9 and the initial quantum number is $n_\mu=3$. One observes that there are two solutions to eq. 6o.

Fig. 5 Fission barrier and the square of the quantum mechanical channel function $u_\mu(x)$ for an incoming wave in the channel $\mu=2$. The parameters are those of eq.(9), $\alpha=0.1$, E = 6 MeV.

Fig. 6 Penetrabilities $P_{\nu\mu}$ for different values of the coupling constant α. The lines correspond to the quantum mechanical coupled channel calculations (solid line for diagonal and broken lines for off-diagonal transitions) and the dots correspond to semiclassical calculations using the uniform Bessel-approximation. The parameters of the potential are given in eq.(9).

Fig. 7 Quantum mechanical transition probabilities versus the coupling strength α for several transitions for the sudden limit case; a) for the reflected waves, b) for the transmitted waves. The parameters are given in the text.

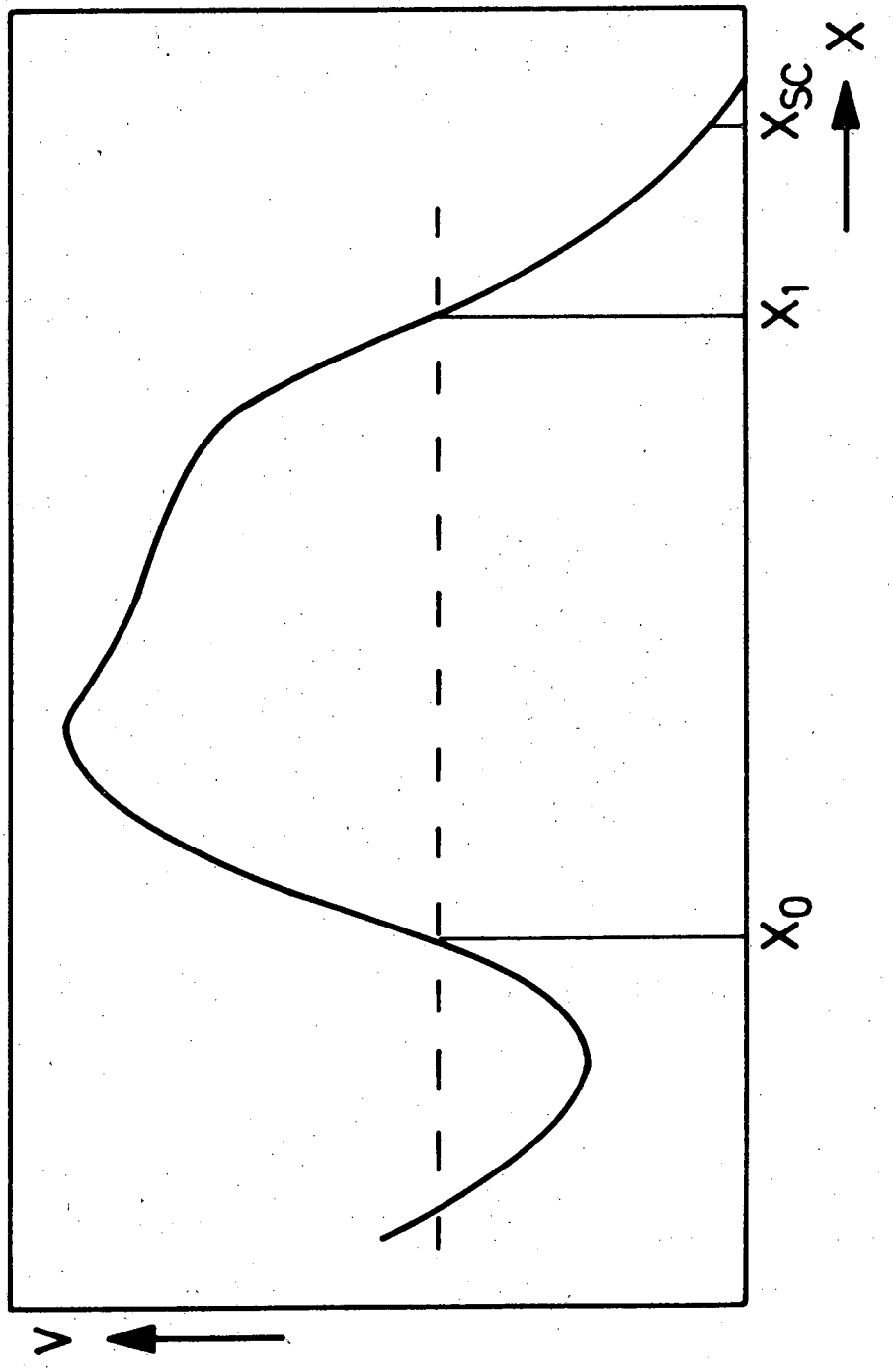

XBL 776-9152

Fig. 1

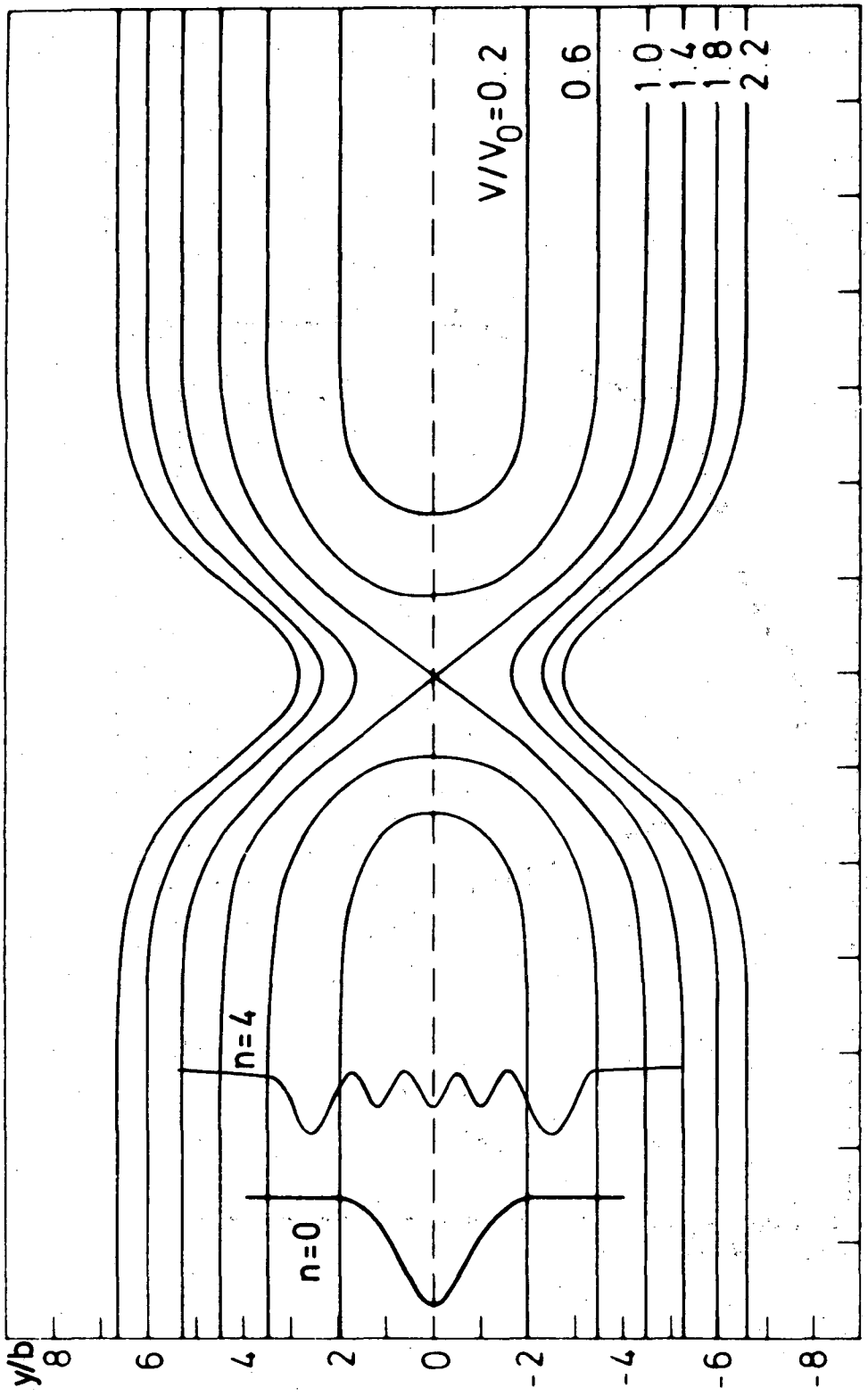

XBL 776-9153

Fig. 2

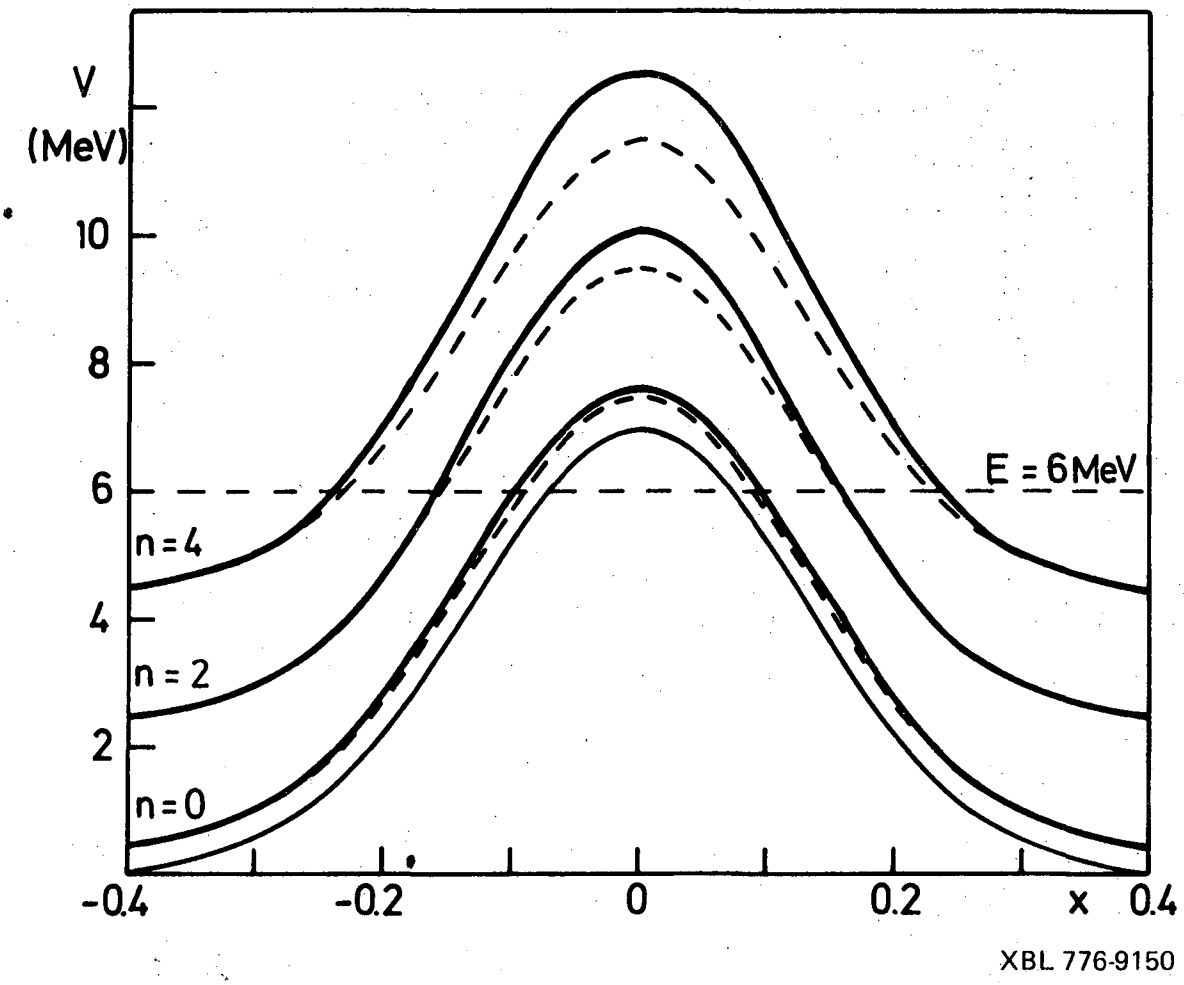

Fig. 3

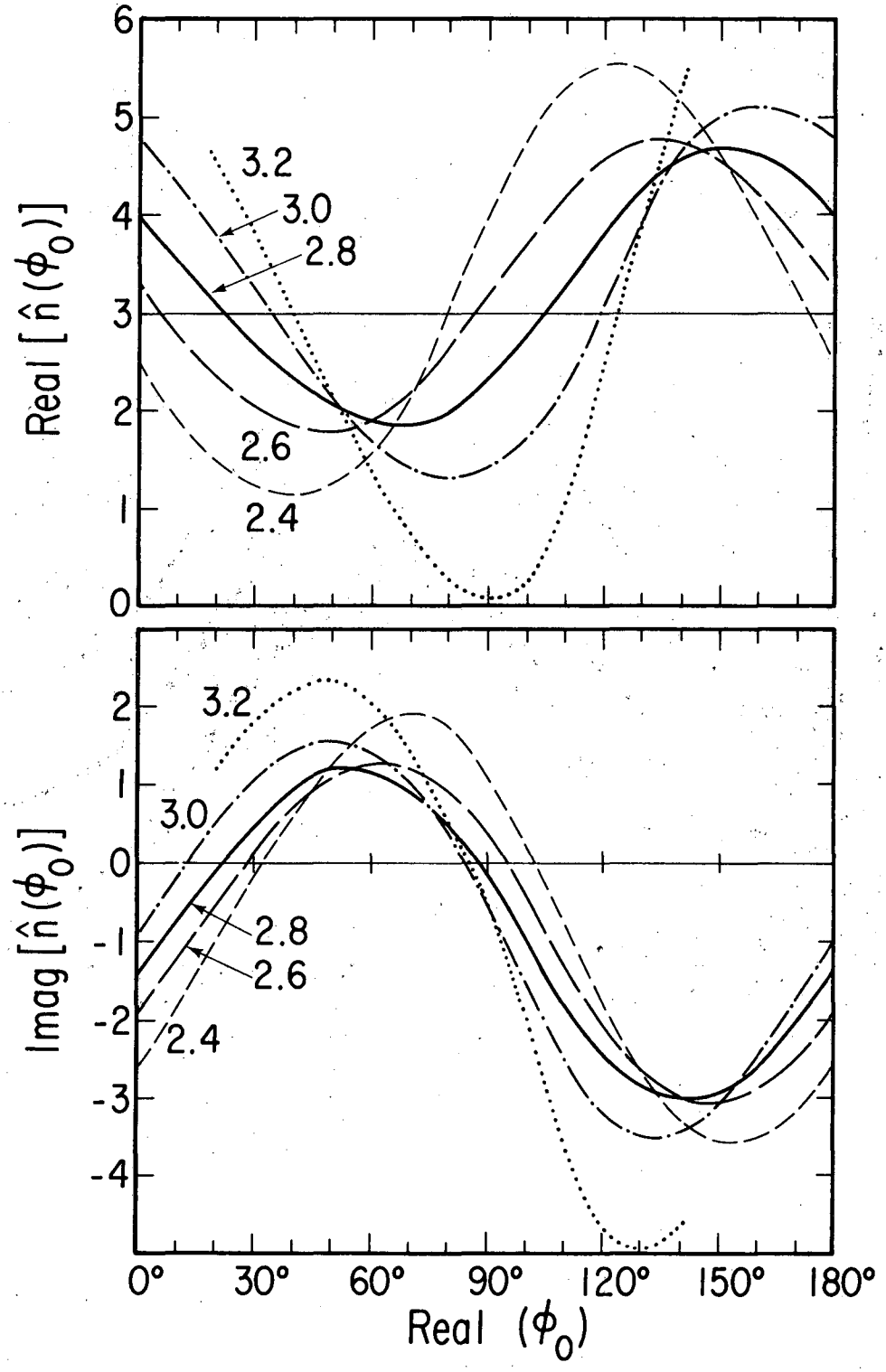

XBL 7510-8405

Fig. 4

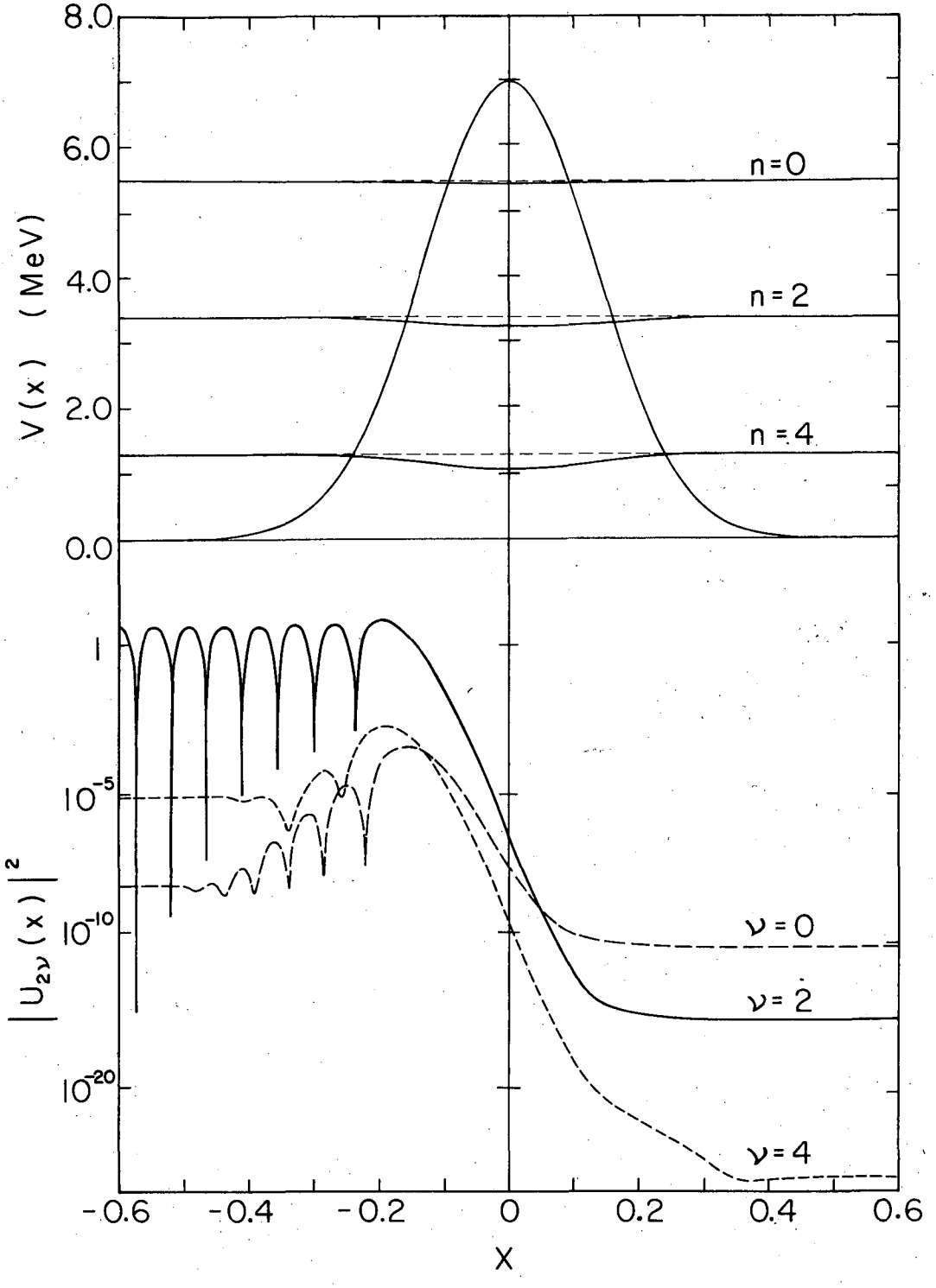
8.0
6.0
4.0
2.0
0.0
V(x) (MeV)
n=0
n=2
n=4
1
10^{-5}
10^{-10}
10^{-20}
$|U_{2\nu}(x)|^2$
ν=0
ν=2
ν=4
-0.6
-0.4
-0.2
0
0.2
0.4
0.6
X
XBL755-2883

Fig. 5

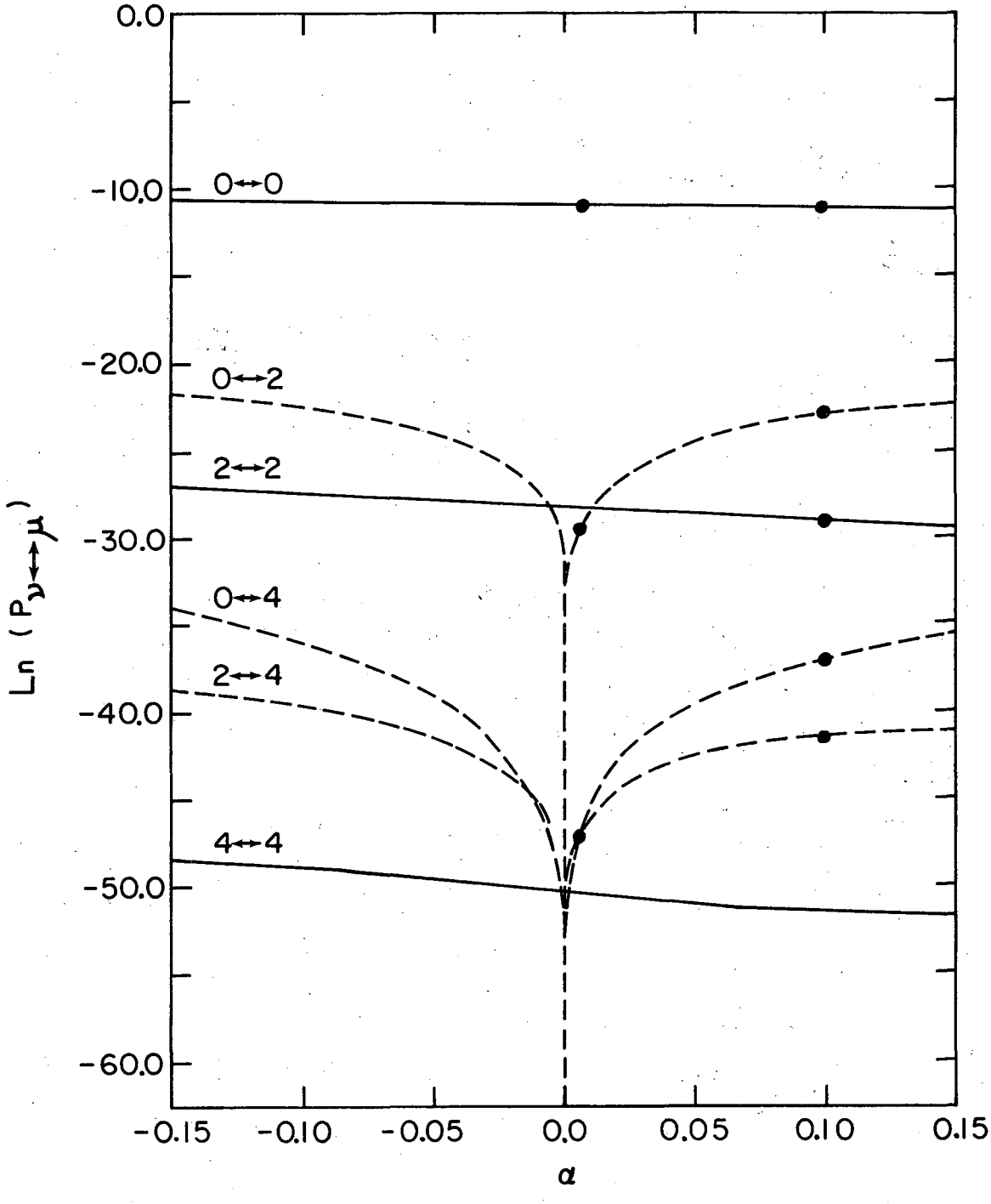
0.0
-10.0
-20.0
-30.0
-40.0
-50.0
-60.0
0↔0
0↔2
2↔2
0↔4
2↔4
4↔4
Ln ($P_{\nu\leftrightarrow\mu}$)
-0.15
-0.10
-0.05
0.0
0.05
0.10
0.15
α
XBL755-2884

Fig. 6

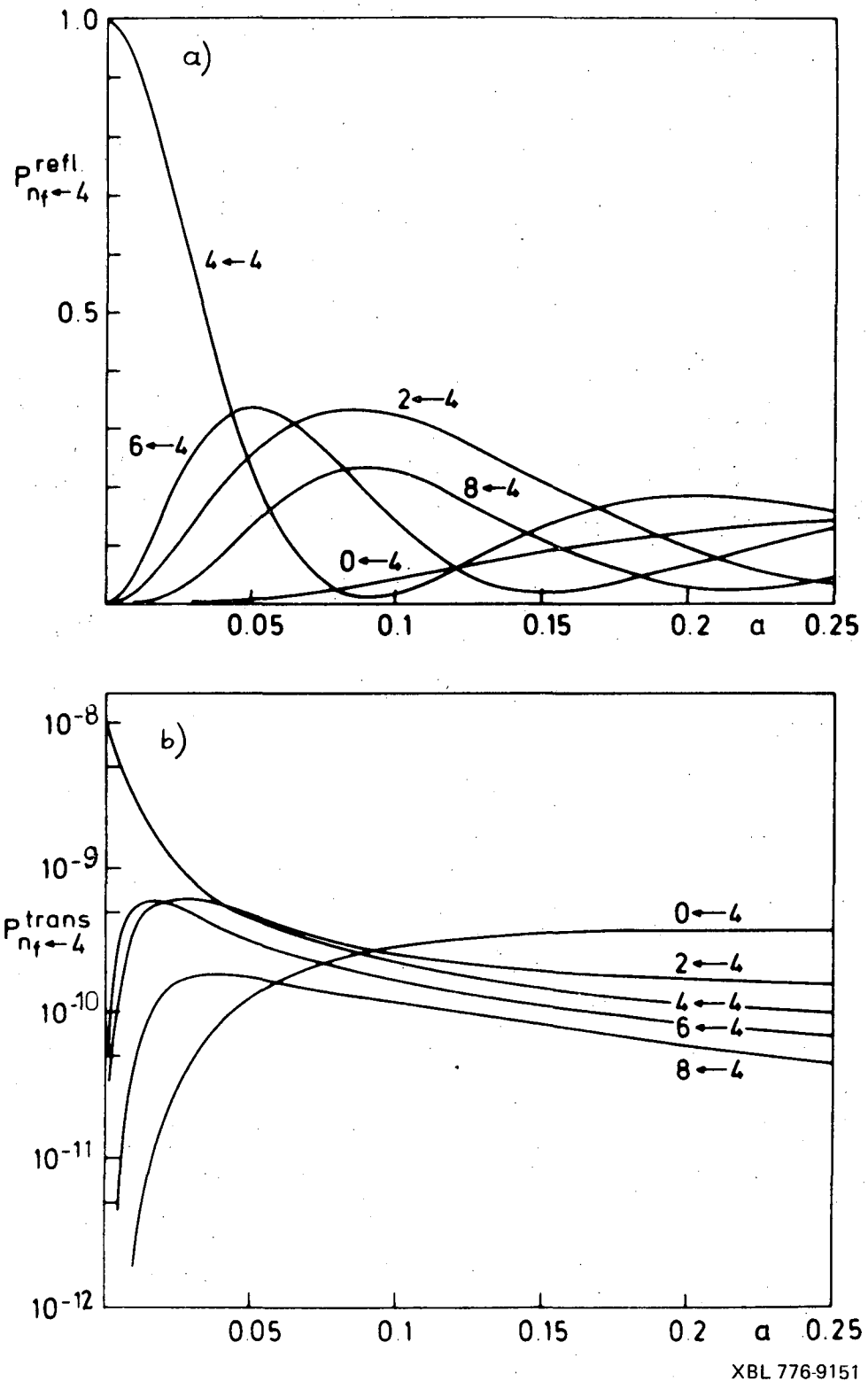

Fig. 7

TECHNICAL INFORMATION DIVISION
LAWRENCE BERKELEY LABORATORY
UNIVERSITY OF CALIFORNIA
BERKELEY, CALIFORNIA 94720